Available online at www.sciencedirect.com
SCIENCE DIRECT®
Journal of Electroanalytical Chemistry 550–551 (2003) 113–124
Journal of Electroanalytical Chemistry
www.elsevier.com/locate/jelechem

Conformations of an amino–amido–thiolate self-assembled layer on gold in air and in electrolytes

Alexander M. Bittner [a,b,*], Maximilian Epple [a], Klaus Kuhnke [a,b], Raymond Houriet [c], Andreas Heusler [d], Horst Vogel [d], Ari P. Seitsonen [b,e], Klaus Kern [a,b]

[a] Institut de Physique des Nanostructures, EPF Lausanne, CH-1015 Lausanne, Switzerland
[b] Max-Planck-Institut für Festkörperforschung, Heisenbergstr. 1, D-70569 Stuttgart, Germany
[c] Laboratoire de Technologie des Poudres, EPF Lausanne, CH-1015 Lausanne, Switzerland
[d] Institut de Sciences Biomoléculaires, EPF Lausanne, CH-1015 Lausanne, Switzerland
[e] Physikalisch-chemisches Institut, Universität Zürich, Winterthurerstr. 190, CH-8057 Zürich, Switzerland

Received 27 August 2002; received in revised form 15 January 2003; accepted 28 January 2003

Abstract

The amino–amido–thiol AT ($HS–(CH_2)_{10}–CO–NH–CH_2–CH_2–NH_2$), adsorbed on Au(111), was studied by sum frequency generation (SFG) and infrared reflection absorption spectroscopy in the CH_2 stretching vibration region. The SFG and infrared spectra are qualitatively similar; both show the symmetric stretching band and an intense and unusually broad antisymmetric stretching band. The infrared spectra show a reversible difference between a sample dried after rinsing in electrolyte and dried after rinsing in ethanol, thus exhibiting a 'solvent memory' effect. SFG spectra demonstrate that the dried samples have a high density of conformational defects. The defects are located in the C_{10} methylene chain. We ascribe them to intermolecular hydrogen-bonding. When the layer is studied by SFG spectroscopy in aqueous solution, even in the presence of coordinating Pd^{2+} ions no vibrational bands are observed in the CH_2 stretching vibration region. This indicates a strongly reduced defect density with a straightened molecular backbone. We ascribe this to the solvation of the amine group; in this case intermolecular bonds play a minor role.

Keywords: Self-assembled monolayers; Amino–amido–thiol; Au(111) electrode; Sum frequency generation spectroscopy; Infrared reflection absorption spectroscopy

1. Introduction

Self-assembled monolayers (SAMs) of thiolate on gold are model adsorbate systems for which the bond to the substrate (gold) is strong (typically 126 kJ mol^{-1} [1]). Layers with different functional groups can be prepared and the influence of this group can substantially modify the properties of the surface and also the electrochemistry [2]. This makes thiols almost ideal substances to produce chemically modified electrodes. Especially when a well-defined electrode is required, gold single crystals and alkanethiols or ω-modified alkanethiols can be employed. The stability of a SAM in different solvents and electrolytes is crucial for potential applications, but also for in-depth investigations. An example is the stability of alkanethiolate SAMs during electrodeposition of copper [3–5].

In many cases a simple model is assumed: the head group chemisorbs to the substrate surface, a straight backbone points (roughly) in the direction of the surface normal, and functional end groups form the outer SAM surface, see e.g. Ref. [6]. All three assumptions can be wrong, and many (electro)chemical and physical properties of a SAM are heavily influenced by defects. Hence, the presence and nature of defects will determine whether or not a SAM is suitable as a building block for more complex structures. While defects that allow a penetration of the SAM will strongly influence the electrochemical behavior [3], more subtle changes are found in the molecular conformation. The energies involved are of the order of several kJ mol^{-1}, so the

* Corresponding author.
E-mail address: a.bittner@fkf.mpg.de (A.M. Bittner).

0022-0728/03/$ - see front matter © 2003 Elsevier B.V. All rights reserved.
doi:10.1016/S0022-0728(03)00136-0

mere contact with electrolytes and electrochemical reactions can produce these conformations [3,5,7]. Even non-functionalized alkanethiolate SAMs can change their conformation upon contact with electrolytes [8] and upon change of the electrochemical potential [4,7]. It is known that functionalized thiolate SAMs can respond to their chemical environment by assuming different conformational structures. A good example is an alkoxy-terminated SAM that was shown to be ordered in air, but disordered in D_2O and CCl_4 due to solvent penetration [9].

In this study we will focus on conformational defects in the backbone and end group of the amino–amido–thiol AT, $HS–(CH_2)_{10}–CO–NH–CH_2–CH_2–NH_2$, 11-mercaptoundecanoic acid-*N*-(2-aminoethyl)amide, adsorbed on Au(111) (Fig. 1). We use vibrational spectroscopy to derive structural (conformational) information and employ Fourier transform infrared reflection absorption spectroscopy in air and sum frequency generation (SFG) in both air and aqueous solution. Calculations of the C–H vibrational bands help to assign the observed bands. The functional group of AT was chosen in order to allow hydrogen-bonding between neighboring molecules (which is impossible for alkoxy groups [9]), and also the formation of chelate complexes with Pd^{2+} as a precursor for metal cluster formation on SAMs [10]. Scanning tunneling microscopy proved that a flat and continuous layer was formed [10]. Interchain hydrogen-bonding was assumed to cause a rigid structure.

We aim at proving that the picture of nicely ordered thiolate chains, and especially that of all-*trans* methylene chains $(CH_2)_n$, collapses as soon as functional groups are present. SFG was found to be an ideal method to prove this. In aqueous solvents, neither the aminoethylamide group nor the alkyl backbone of the monolayer generates an observable SFG signal. In contrast, a strong signal from CH_2 stretching vibrations is found by SFG for a dried AT monolayer exposed to air. Both the antisymmetric CH_2 stretching vibration ν_{as} (d^-) and the symmetric stretching vibration ν_s (d^+) are present. Repeated in situ investigation and investigation of the dried layer demonstrate that the SFG intensity reappears reversibly in air. Extending the study to infrared reflection absorption spectroscopy (IRRAS) from dried samples, we find that spectra in air are different, depending on whether a sample was rinsed in aqueous electrolyte or in ethanol before recording a spectrum: the dry layer has a 'memory' of the last solvent.

The paper is organized as follows: in Section 2 the sample preparation and the experimental methods are introduced. The results are presented in Section 3. Section 4 presents an estimate of SFG signals and several simple spectral calculations. In Section 5 we analyze and discuss the shapes, bandwidths, and intensities of the spectra. Section 6 summarizes the work.

2. Experimental

AT and partially deuterated AT, $HS–(CH_2)_{10}–CO–NH–CD_2–CD_2–NH_3^+$ CF_3COO^-, were synthesized according to standard procedures. Samples were prepared by immersion of Au(111) single crystal surfaces or (111)-oriented gold films in 20 μM ethanolic solutions of AT for 12–48 h at 325 K. The films were evaporated on mica (base pressure 2×10^{-6} mbar, 120 nm gold on 550–560 K hot mica, 3 h annealing at 620 K, flame annealing). For most infrared spectra, the substrate was gold sputtered on glass. The samples were investigated after rinsing with flowing ethanol (p.a., Fluka). Alternatively, they were investigated during (SFG experiments) or after (SFG/IRRAS experiments) exposure to a Pd^{2+} solution of 0.7 mM Na_2PdCl_4 (Aldrich) and 0.7 M NaCl (Fluka) in water (MilliQ), adjusted to pH 1 with HCl (Fluka), referred to as solution **A**. This solution was used in order to allow chelate formation of the functional group with Pd^{2+}. When emersed, the samples were rinsed with 0.1 M HCl+0.6 M NaCl (solution **B**). In some cases, further rinsing in ethanol followed.

In the SFG spectroscopic set-up [5] a two stage optical parametrical amplifier set-up was used to generate tunable infrared pulses. The system was driven by a Nd:YAG laser that provided 35 ps pulses. In the range from 2750 to 3100 cm^{-1} the energy per infrared pulse was about 100 μJ with a width of 12 cm^{-1}. A part of the doubled fundamental Nd:YAG beam was used as a visible up-conversion pulse (532.06 nm) to generate the SFG signal at the sample.

The visible beam was parallel and p-polarized with an energy density on the sample of about 5 mJ cm^{-2} over a beam diameter of about 3 mm. It impinged at an angle of 62° with respect to the sample normal. The polarization of the infrared beam was also selected to be p-polarized on the sample. It was slightly focused to a beam diameter of about 1 mm on the surface (typical energy density 10 mJ cm^{-2}). The incidence angle with respect to the surface normal was 58°. In the in situ experiments both beams entered an equilateral CaF_2 prism, and the incidence angles at the surface became 70° for the visible and 56° for the infrared beam. The difference in the two geometries resulted in a slightly different field strength of the beams in the adsorbate layer.

The emitted p-polarized SFG signal passed into a monochromator and a photomultiplier, read by a gated charge integrator. The spectral width of the monochromator was set much wider than the bandwidth of the SFG signal determined by the width of the infrared beam, thus inducing no restrictions on spectral resolution. We limited the intensity of the incident beams so that approximately 10 SFG photons per pulse from the

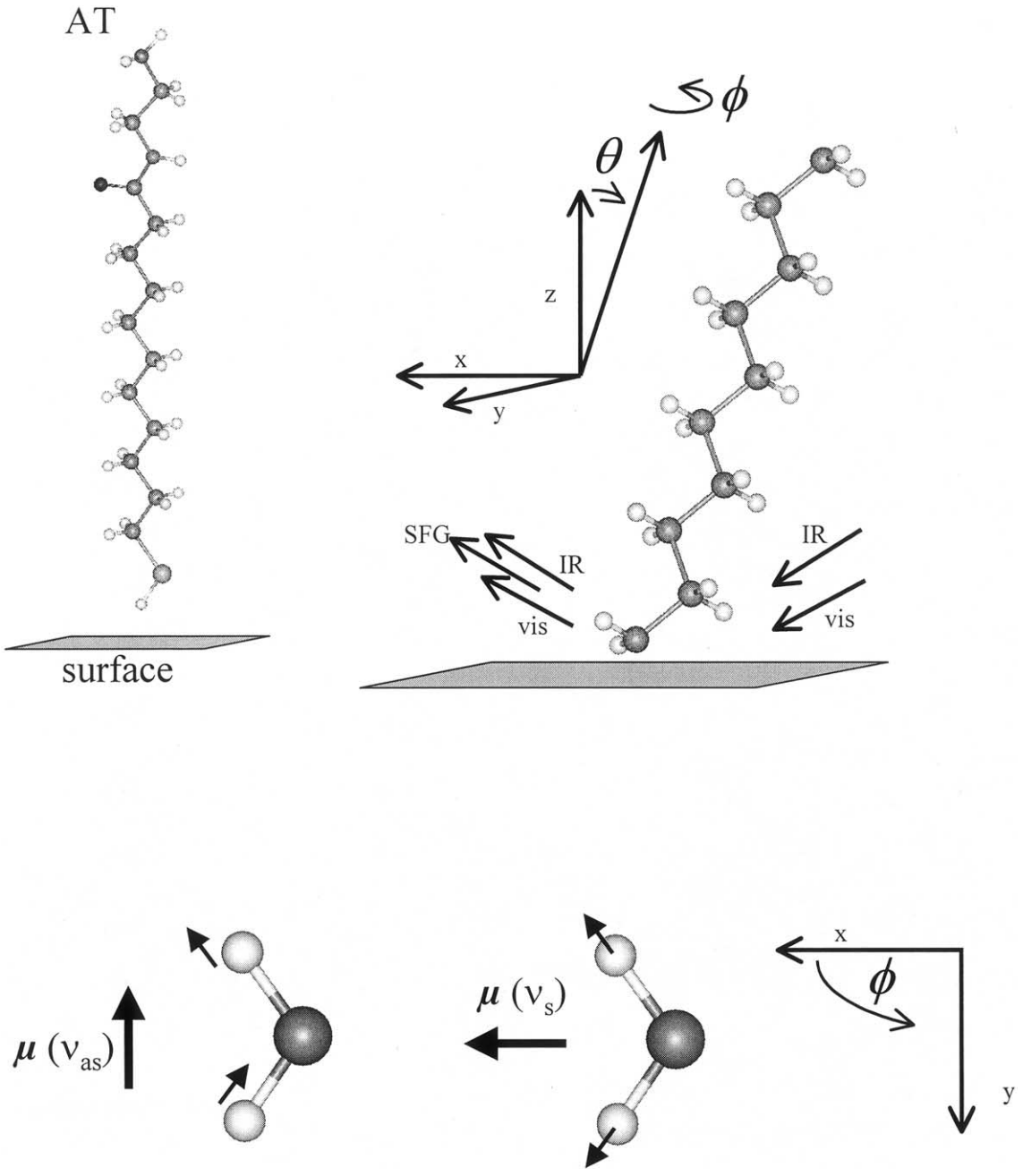

Fig. 1. Experimental set-up and orientation of adsorbed amino–amido–thiol AT ($HS–(CH_2)_{10}–CO–NH–CH_2–CH_2–NH_2$). (a) Molecule; (b) definition of angles and axes of the molecular backbone: θ = tilt of alkyl chain from surface normal, ϕ = rotation around molecular axis, gold surface = xy plane, plane of incidence of the light beams = xz; (c) transition dipole moments $\boldsymbol{\mu}$ of CH_2 stretching vibrations (s, symmetric; as, antisymmetric). Here a CH_2 group (pointing to the left in (b)) is shown in top view for $\theta = \phi = 0°$.

Au substrate were measured. No degradation of the thiolate layer was observed after several hours of measurements.

The spectral resolution of the SFG measurement was determined by the spectral width of the infrared pulses, which was chosen to be 12 cm^{-1}. The angular tuning of the non-linear crystals can induce systematic errors which were determined daily by placing a styrene foil into the beam path of the tunable infrared beam and measuring an absorption spectrum between 2800 and 3150 cm^{-1} with a pyroelectric pulse energy meter as a detector. Comparison with an infrared spectrum of the same foil gave a daily wavenumber correction that we estimated to be precise to within ± 2 cm^{-1}. The procedure worked well in a previous study of CH_3 stretching vibrations [5]. For in situ measurements we corrected for the background [5].

Infrared measurements shown in this paper were performed with a Mattson Galaxy 6020 FT-IR spectrometer in air. Purely p-polarized light was collected from

the sample with an 80° grazing incidence accessory (Spectratech). The detector was a liquid-nitrogen-cooled mercury cadmium telluride detector. The resolution was 5 cm^{-1} and the scanned energy range 1900–3500 cm^{-1}. The measuring time per spectrum was about 10 min for 400 averaged scans. The reference sample was ethanol-rinsed gold.

2.1. Theoretical calculations

We performed density functional theory (DFT) calculations for the frequencies and infrared intensities in $HS–(CH_2)_{10}–CO–NH–CH_2–CH_2–NH_2$, $HS–(CH_2)_{10}–CO–NH–CD_2–CD_2–NH_2$, n-C_nH_{2n+2}, $D–(CH_2)_n–D$ and $D_3C–(CH_2)_{n-2}–CD_3$, $n = 1,\ldots, 9$, and for cyclo-C_nH_{2n}, $n = 3,\ldots, 7$. The calculations were done using the program GAUSSIAN98 [11] and employing LDA as the exchange-correlation functional. We chose the large 6-311G(d,p) basis set for the alkanes and 6-311+G(2df,2pd) set for the AT. The calculations were tested for convergence in the basis set. We also checked that the results were consistent for splitting and intensity by comparing the DFT results with explicitly correlated quantum chemistry methods MP2 and CISD with the basis set 6-311++G(3df,3pd). We obtained the frequencies and infrared intensities via the harmonic approximation. Combined with the approximate exchange-correlation functional, this leads to a certain, well-known error in the frequencies which is systematic. Hence, we are convinced of the correctness of the trends and qualitative results.

3. Results

3.1. Sum frequency generation in situ/ex situ

Fig. 2 shows SFG spectra taken for dried samples in air after rinsing in ethanol (a) and after contact with Pd(II)-containing solution **A**, followed by rinsing in water (b). The presence of Pd(II) does not obviously cause substantial changes: both spectra exhibit two vibrational bands which appear as negative peaks [5,12] on a dominant Au surface signal which was normalized to 1. The bands are assigned to the symmetric and antisymmetric CH_2 stretching vibration, ν_s (d^+) and ν_{as} (d^-). We obtained very similar spectra for other SAMs that contain CH_2 (but no CH_3) groups [13]. Literature values in infrared spectroscopy are 2850 and 2920 cm^{-1}, respectively, while better ordering results in slightly lower energies around 2848 and 2915 cm^{-1} [14–18]. The corresponding energies found in Raman spectroscopy are 2850 and 2880 cm^{-1} [19–24], where a broad background and many additional peaks can be attributed to the stretching vibrations, too. Literature values of SFG methylene resonances are very close to those known from infrared spectra [25], see also Table 1.

Fig. 3 shows SFG spectra of a freshly prepared sample in air (a), in chloropalladate solution **A** (b), and—after a rinse in solution **B**—again in air (c). The resonances disappear in the solution, and this was also confirmed for the Pd(II)-free solution **B**. They reappear when the sample is dried again, which demonstrates that the disappearance of the bands is not due to desorption. The Fresnel factors (i.e. the coupling between the external field and the field in the layer) do not change significantly between the two geometries, hence a comparison of the intensities is justified. Note that in solution only the resonances disappear while the substrate signal remains strong.

We searched for an SFG signal specifically from the amine and amide groups scanning the NH stretching region between 3100 and 3600 cm^{-1} carefully in co-propagating (infrared and visible beams incident almost parallel to each other, see Section 2) and counter-propagating geometry (infrared and visible beams incident from opposite directions). No peaks were found in the spectra, demonstrating that the intensity of the NH stretching vibration must be smaller than a few percent of the Au substrate signal.

3.2. Infrared reflection absorption spectroscopy ex situ

In order to extend the study we recorded IRRAS spectra (Fig. 4) for similar preparations. Spectra found after rinsing with water, with solution **B** or with the chloropalladate solution **A** did not differ substantially (as for SFG, see Fig. 2). Similarities and differences between infrared and SFG spectra and the differences in sensitivity of the two methods will be discussed in Section 5. A feature found most clearly in the infrared spectra is the appearance of a weak additional peak near 2960 cm^{-1} which can, with some difficulty, also be found in the SFG spectra (Fig. 2b). We term this peak a 'defect peak'. Attenuated total reflection infrared spectra of identically prepared samples confirmed these results.

We found that the intensity of the stretching vibrations and especially of the 'defect peak' depends on the solvent or electrolyte used before drying. A freshly prepared AT SAM, rinsed in water, in 1 M NaCl or in Pd(II)-free solution **B**, clearly exhibits the 'defect peak', in contrast to the spectrum before the rinsing procedure (see Fig. 4). Surprisingly, re-immersion in pure ethanol or in AT+ethanol resulted in spectra that again resembled those of freshly prepared films. (We found that the difference between the two

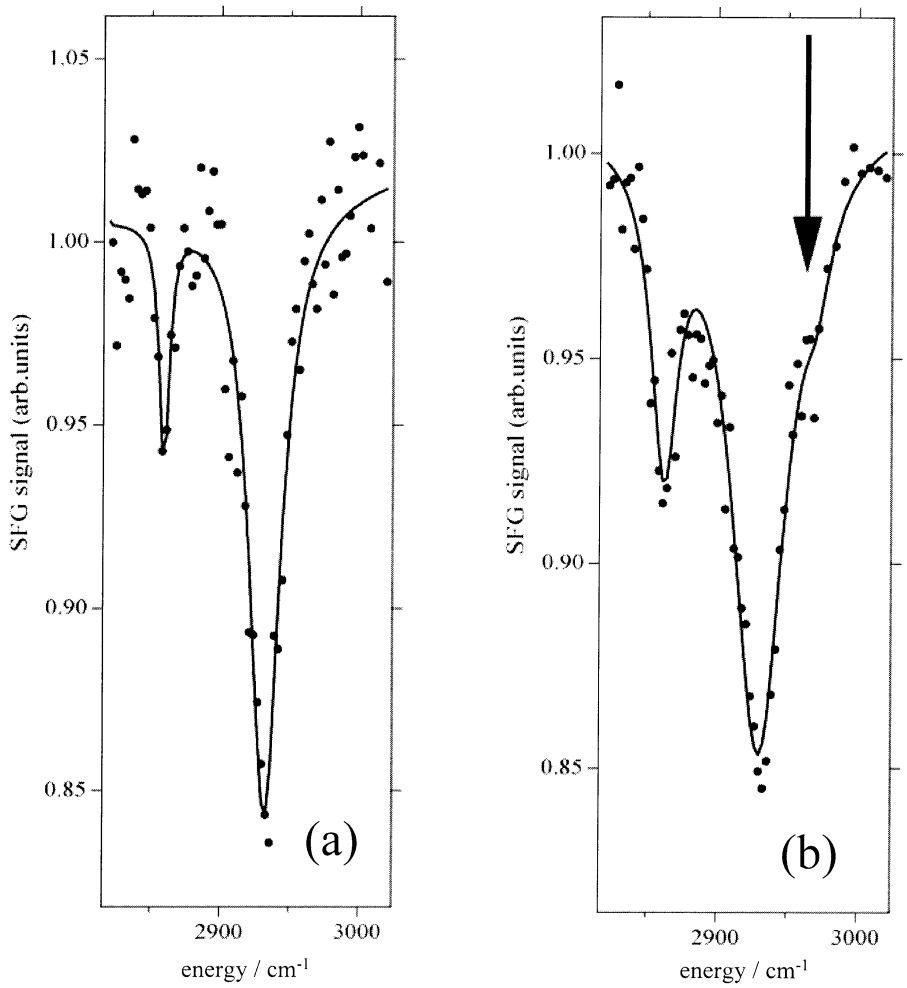

Fig. 2. SFG spectra of samples dried in air. (a) Sample after preparation taken out of ethanolic solution and rinsed in ethanol; (b) sample after preparation with Pd^{2+} (see text) and rinsing in water. The arrow shows the position of the 'defect peak' (see text). The full points are the measured data, the solid lines are best fits of Lorentzian lines whose parameters are given in Table 1. Nearly identical spectra were found for AT with a deuterated end group, $CO–NH–CD_2–CD_2–NH_2$.

spectra was greater after rinsing with NaCl solution in comparison to rinsing with water.) The intensity of the CH_2 groups increases by $>50\%$ after exposure to aqueous electrolyte and drying, while the 'defect peak' increases by about a factor of four (see Fig. 4). This is reversible and can be repeated in any order. We term this behavior the 'solvent memory effect'.

4. Spectral analysis

4.1. SFG and infrared intensities for the CH_2 stretching modes

For well-ordered alkanethiolates and similar systems, the vibrations of the CH_2 groups are extremely weak or

Table 1
AT ($HS–(CH_2)_{10}–CO–NH–CH_2–CH_2–NH_2$) methylene stretching resonance energies ('pos'), bandwidths (FWHM), and relative peak amplitudes obtained from the best fits shown as solid lines in Figs. 2 and 4

Method/sample	Symmetric C–H stretch ν_s (CH_2), d^+			Antisymmetric C–H stretch ν_{as} (CH_2), d^-			'Defect peak'		
	Pos/cm^{-1}	Width/cm^{-1}	Rel. ampl.	Pos/cm^{-1}	Width/cm^{-1}	Rel. ampl.	Pos/cm^{-1}	Width/cm^{-1}	Rel. ampl.
SFG AT	2859	9(?)	$0.066^{(s)}$	2932	27	$0.171^{(s)}$	–	–	–
SFG AT (Pd)	2862	23	$0.076^{(s)}$	2930	47	$0.157^{(s)}$	2971	23 (!)	$0.017^{(s)}$
Infrared AT	2856	28	$0.108^{(a)}$	2924	34	$0.320^{(a)}$	2959	29	$0.030^{(a)}$
Infrared AT (Pd)	2858	32	$0.206^{(a)}$	2926	37	$0.529^{(a)}$	2963	18	$0.120^{(a)}$

For SFG the amplitude is normalized to the substrate signal of $Au^{(s)}$, for IRRAS the given value is the absorbance$^{(a)}$; these two scales have different units and cannot be compared directly. The (?) marks a peak width which must be doubted because it is narrower than the experimental resolution. The (!) marks a width that was guessed and could not be varied in the fitting procedure.

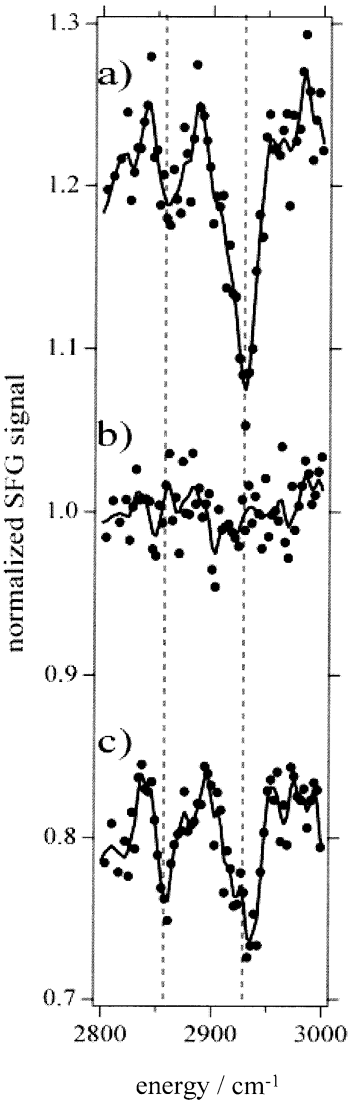

Fig. 3. Series of normalized SFG spectra for the same sample: (a) prepared in ethanolic AT solution, rinsed in ethanol and dried; (b) in situ in aqueous chloropalladate electrolyte; (c) emersed, rinsed with NaCl+HCl solution and dried. The curves (a) and (c) are offset for clarity. The series demonstrates that the CH_2 stretching vibrational bands disappear in solution even though the layer does not desorb. The points are the measured data corrected for background slope; the lines are the smoothed data.

not observed in SFG [7,25–27]. Two conditions have to be fulfilled in order to make their observation possible: first, the inversion symmetry of the alkyl chain must be broken, e.g. due to an odd number of CH_2 groups or due to a deviation from the all-*trans* conformation [9,25,26]. The second condition—which also applies to IRRAS—is that a sufficiently large number of CH_2 groups are oriented such that both the antisymmetric and symmetric modes generate an SFG signal. This forbids the following three local orientations: H–C–H plane nearly parallel to the surface, –C–C–C– plane perpendicular to the plane of incidence, –C–C–C– plane parallel to the plane of incidence (see also Fig. 1).

In our earlier investigation of alkanethiolate layers [5] we utilized an oversimplified model which is based on the linear superposition of $\chi^{(2)}$ tensors, assigned to the vibrational motion of one C–H bond. We thus determined the CH_3 orientation of alkanethiolates. A similar calculation is not fruitful for this study since the relative SFG intensities of ν_s and ν_{as} are not strongly dependent on tilt and twist angles. The extreme bandwidth of ν_{as} makes it difficult to assign a meaningful value to the average orientation of the methylene groups.

However, we can roughly estimate the density of observed CH_2 groups by comparison to our alkanethiolate study [5]. The intensities are determined by the orientation and possible differences in the molecular density. For well-ordered octadecanethiolate on gold, the measured CH_3 antisymmetric stretching mode intensity is 20% of the Au substrate signal. The calculated intensity is around 0.015 units. The measured CH_2 antisymmetric stretching mode intensity is 15% of the Au substrate signal. The calculated intensity assumes a maximum value of 0.2 units. Assuming that the substrate signal is the same in both cases (differences may be due to the different sulphur concentrations at the surface) we obtain that the observed CH_2 group density is a factor of three smaller than the CH_3 group density in octadecanethiolate. Due to the three times larger bandwidth found for AT compared to octadecanethiolate, however, we underestimate the density of the observed CH_2 groups by approximately this factor. Moreover one can assume that the molecular density of the AT layer is smaller than for long chain alkanethiolates. We can thus estimate that we observe on average one CH_2 group per molecule in a favorable orientation for SFG (or several groups in less favorable orientations).

4.2. Comparison of CH_2 stretching modes with calculated and literature values

In this section we would like to compare our spectra with alkane bulk spectra and with calculated infrared spectra of free AT and alkane molecules (Fig. 5 and Table 2). Our model calculation provided the experimentally observed vibrational resonances with an offset of roughly $+50\ cm^{-1}$. The calculated AT spectra agree with the measured ones although only the latter refer to a monolayer. The ν_s (d^+) and ν_{as} (d^-) bands comprise each a group of eigenmodes of the appropriate symmetry, closely spaced in frequency. Two features in the calculated AT spectra are surprising: first, the deuteration showed that the methylene stretching vibrations of the aminoethylamide overlap with those of the alkyl backbone. This means that deuteration merely changes the intensities of these vibrations, in perfect agreement

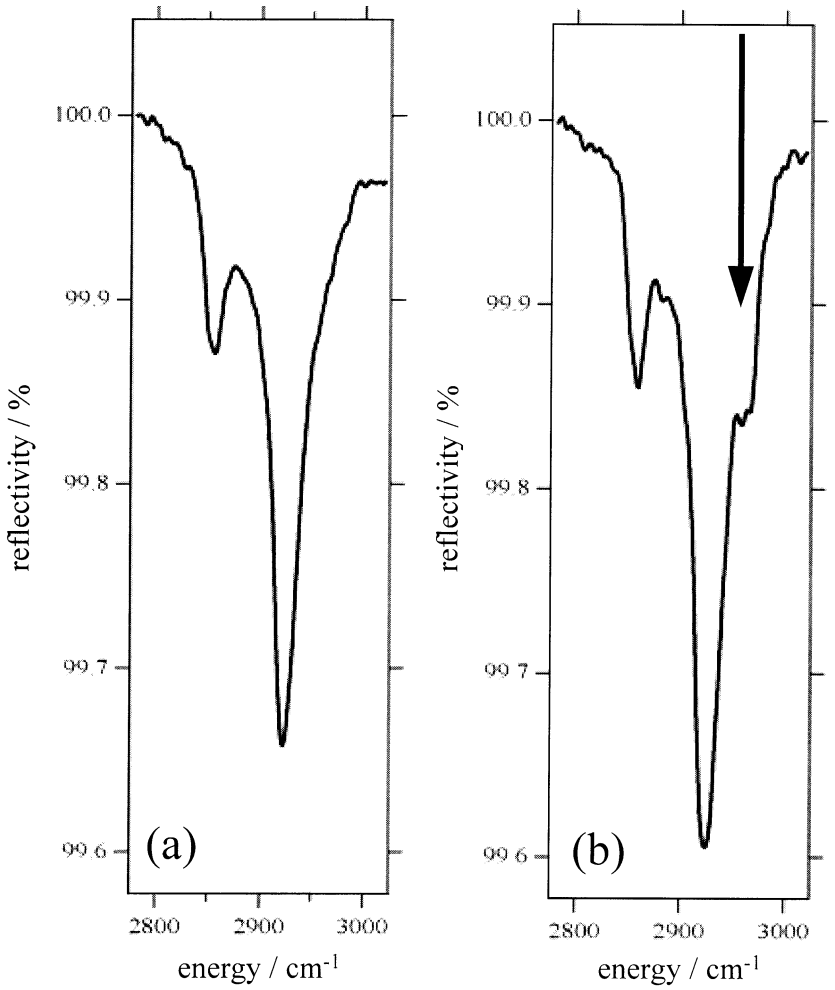

Fig. 4. Infrared reflection absorption spectra of samples dried in air. (a) Sample after preparation as taken out of ethanolic AT solution and rinsed in ethanol; (b) sample after rinsing with NaCl+HCl solution. The arrow shows the position of the 'defect peak' (see text). The spectra of Fig. 5 show similar peak parameters as Fig. 4. The full points are the measured data, the solid lines are best fits whose parameters are given in Table 1. Nearly identical spectra were found for a deuterated end group, $CO–NH–CD_2–CD_2–NH_2$.

with the experiment. Second, some additional weak bands were found at 2910, 2915, 2950 and 2965 cm^{-1}. They are due to C–H stretching of the two or three methylene groups adjacent to the CO and SH groups. The high frequency bands could possibly explain the 'defect peak' in our experimental spectra, but further theoretical studies on related molecules are required to confirm this.

For the calculated alkane infrared spectra we eliminated the CH_3 resonances by deuteration to CD_3. Note that CH_2D is not sufficient since $\nu(CH_2)$ in the methyl group is shifted in frequency and produces new bands. A comparison with the literature on infrared vibrational frequencies shows that we can reproduce the CH_2 bands well, and the relative intensities very well. Again the ν_s (d^+) and ν_{as} (d^-) bands each comprise a group of eigenmodes of the appropriate symmetry, closely spaced in frequency. In addition, we find several symmetric modes 10–25 cm^{-1} below ν_s, which have not been observed experimentally, presumably due to their low intensities.

The simulation of typical conformational defects was attained by starting with an alkyl backbone with a single gauche defect (local energy minimum) or with a gauche–*trans*–gauche (kink) sequence. Results are similar to the alkane results shown in Fig. 5 and Table 2. In all cases the bands were located close (10 cm^{-1}) to our experimental values, $\sim$2850 and 2920 cm^{-1}. In a first approximation our infrared experimental results are consistent with trans as well as gauche structures. Including finer details, the slight blue shifts (+9 and +5 cm^{-1}) of the bands compared to long-chain alkanethiolates (see Tables 1 and 2) are compatible with some disorder, often interpreted as gauche defects. Such values are commonly observed for shorter alkanethiolate SAMs which are known to be less ordered

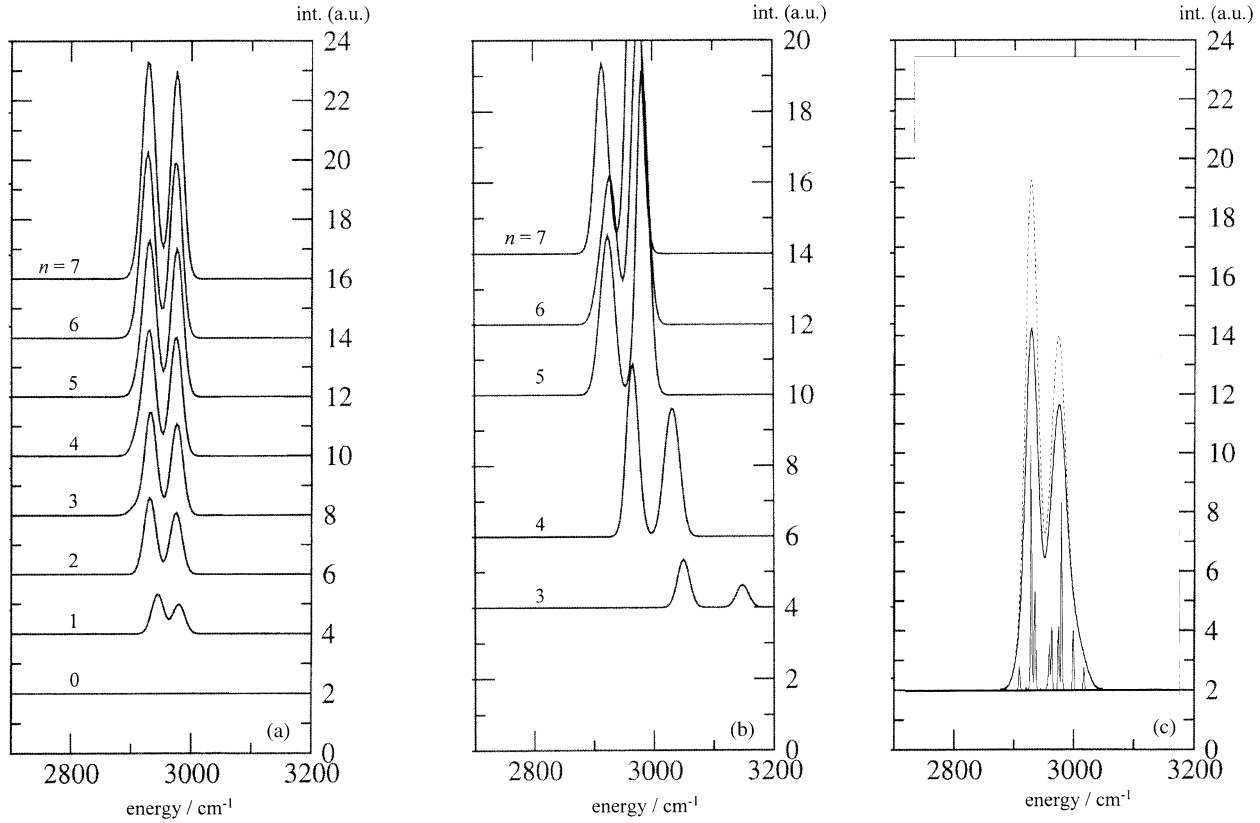

Fig. 5. Calculated infrared spectra, offset for clarity, plotted with an FWHM peak width set to 23.6 cm^{-1}. (a) Spectra for methylene chains with n C atoms, CD_3–$(CH_2)_n$–CD_3; the end groups were deuterated to suppress methyl resonances. The all-*trans* chains—even chains with slight conformational defects (gauche) (not shown)—show typical methylene vibrations. (b) Stronger deformations from gauche to *cis* are simulated with the help of cyclic alkanes $(CH_2)_n$. (c) Spectra for the free deuterated AT molecule (end group CO–NH–CD_2–CD_2–NH_2). At bottom: the same spectrum plotted with 2.36 cm^{-1} FWHM. Dashed: not deuterated.

[1,3]. Note that also the aminoethyl end group shows these bands (liquid ethylene diamine: 2857 and 2920 cm^{-1} [28]). In contrast, a typical bidentate ethylenediamine-type Pd(II) complex [29,30] and an amino acid-type complex [31] both exhibit large blue shifts (>30 cm^{-1} for each band). Thus we find no indication for this type of complex (it may still be present, but not as majority species).

Whether the assumption of gauche defects is indeed justified, can only be answered by model systems with energetically less favored defects, in the extreme case *cis* (eclipsed). To determine the vibrational frequencies at *cis* defects, which cannot be easily simulated because this conformation corresponds to an energy maximum in alkanes, we used a trick to study the frequencies of cycloalkanes (see Fig. 5 and Table 2). As can be expected, only the small rings C_n ($n<6$) behaved much differently from *n*-alkanes. Due to their near-planar geometry, adjacent C–H bonds in small rings are situated in a *cis*-eclipsed or nearly eclipsed ('near-*cis*') position. This results in significant blue shifts (>20 cm^{-1}) of both methylene stretching bands which we do not observe in AT.

Medium-sized rings show a much better fit; the best is cyclohexane which—in its lowest energy 'chair' shape—contains only gauche conformations (cycloheptane is a similar case). It is important that the principal character of the bands is preserved in all cases, i.e. all alkanes investigated exhibit geometrically closely related C–H stretching modes. We did not find any resonance above the ν_{as} band that might explain our 'defect peak'. The simulated defects lead in some cases also to a broader distribution of the band frequencies. But even this effect can explain only the slight broadening of ν_s, not the extreme broadening of ν_{as}, for which it would be necessary to include vibrational coupling to low-frequency modes.

As a result, our infrared spectra fit well with methylene chains that are composed of multiple gauche conformations such as cyclohexane. This is confirmed by the estimate of one defect (on average) per chain, deduced from our SFG results (see Section 4.1).

Table 2
Methylene stretching resonance energies for AT and for related alkanes [28,37]. For some of the alkanes a calculation was performed for CD_3–$(CH_2)_n$–CD_3 (see Fig. 5)

Method/sample	Pos/cm^{-1}				
	Symmetric C–H stretch ν_s (CH_2), d$^+$	Symmetric C–H stretch calculation[a]	Antisymmetric C–H stretch ν_{as} (CH_2), d$^-$	Antisymmetric C–H stretch calculation[a]	Other bands
SFG AT	2861	–	2931	–	2971
SFG SAM [25]	2855	–	2915	–	–
Infrared AT	2857	2880	2925	2930	2961
Infrared *n*-alkanes C > 4 [28]	2857	2880 (2870)	2920–2928	2925	–
Infrared cyclo-C_8	2850	–	2915	–	–
Infrared cyclo-$C_{6,7}$	2853	2870	2923	2915	–
Infrared cyclo-C_5	2868	2870	2963	2930	2920
Infrared cyclo-C_4	2945	2910	2974	2970	2965

[a] 50 cm^{-1} offset subtracted. The end groups were deuterated to suppress methyl resonances.

5. Discussion

5.1. Assignment of vibrational modes

The two experimentally observed peaks are assigned to the symmetric and antisymmetric CH_2 stretching vibrations, ν_s (d$^+$) and ν_{as} (d$^-$). Empirically, SFG spectra of SAMs are similar to infrared spectra (a green visible beam on gold even results in negative SFG resonances [5,12]). This is well known for the methyl group (infrared: Refs. [14–18], SFG: Refs. [5,7,25–27]). The observed CH_2 vibrations originate from the $(CH_2)_{10}$ chain, not from the ethylene group, as proven by recording spectra of adsorbed HS–$(CH_2)_{10}$–CO–NH–CD_2–CD_2–NH_3^+ CF_3COO^- in which the ethylene group is selectively deuterated. Our calculated infrared spectra of free AT molecules and of the deuterated species verify the observations. *Quantitatively* the same spectra were observed with IRRAS and SFG. We postulate furthermore that a dry AT layer contains a strongly deformed C_{10} alkyl chain, presumably with multiple gauche defects (see Section 4.2).

A closer look at Table 1 reveals a small but significant difference between the SFG and infrared spectra. The observed difference is reproducible and between 4 and 8 cm^{-1} for the antisymmetric mode. The shift becomes even larger if one does not take the fitted band position but the actual peak of the band. This phenomenon is not known for the CH_3 stretching resonances of alkanethiolate SAMs in IRRAS [14–18] and SFG [5,7,25–27]. The antisymmetric stretching vibration exhibits a slightly asymmetric band shape whose asymmetry is reversed with respect to the SFG band shape. The reason is a strong dispersion along the alkyl backbone [21]. This is reflected by the infrared energy (2920 cm^{-1}) that deviates substantially from the Raman energy (2880 cm^{-1}). SFG can observe only modes which are both infrared and Raman active. Such modes can occur only if the inversion symmetry of the backbone is broken. In a naive picture one might then expect SFG intensity all the way between the observed infrared and Raman frequencies. This is, however, not correct because SFG is selective enough to generate a peak at a single frequency where the product of the two contributions reaches a maximum, which is close to the infrared frequency. This is supported by Raman spectra of alkanethiolate SAMs [19,20] and of alkanes [21,28]: a broad background and a large number of peaks occur in the spectral range of C–H stretching vibrations.

The signal at approximately 2960 cm^{-1} is difficult to interpret. We note that a peak at 2960 cm^{-1} is often found in infrared spectra of alkyl-containing compounds where it can be confused with the CH_3 antisymmetric stretch. This is not the case here since no CH_3 groups are present. As we proved with selectively deuterated AT, HS–$(CH_2)_{10}$–CO–NH–CD_2–CD_2–NH_3^+ CF_3COO^-, this 'defect peak' is not due to the aminoethylamide end group since IRRAS results are identical for deuterated and non-deuterated AT. It is situated in the C–H stretching region and is clearly correlated with AT since it is not found in the case of ω-modified thiolate SAMs [17,32]. The band frequency is too low to compare it with aminoacid complexes of Pd(II) [31]. It may fit to ethylenediamine complexes of Pd(II), but then a fourth peak should be visible [29,30]. Moreover, we can rule out the ethylene group with our deuteration experiments. The 'defect peak' appears to occur only in systems with alkyl chain disorder, e.g. in some cases in polyethylene [33]. We thus interpret the peak as characteristic for strongly deformed alkyl chains (more distortion than in gauche defects). Our calculated infrared spectra of AT show C–H stretching modes from methylene groups adjacent to the CO and SH group at 2950 and 2965 cm^{-1}. It is possible that some of these modes increase in intensity upon chain deformation. A related example could be a similar IRRAS band of an alkanethiolate with an SO_3H terminal group [34][1].

5.2. Widths of the vibrational bands

Bandwidths are determined by lifetime broadening, dephasing and inhomogeneous broadening. A simple theoretical evaluation demonstrates that infrared and SFG homogeneous bandwidths should be identical because both contain the same infrared resonance denominator (in the approximation of weak absorbance). Also dominant inhomogeneous broadening gives a similar width (numerical calculation with a Gaussian broadening shows that SFG peaks are some 15% broader (FWHM) than infrared resonances).

Surprisingly, we find that the ν_{as} mode in SFG and infrared spectra is much broader than the ν_s mode. Note that AT in this respect is different from a thiolate SAM with a carboxylate end group where the widths are approximately 15 (s) and 25 cm^{-1} (as) [17]. The band asymmetry, which is evident for the antisymmetric stretching mode, suggests some inhomogeneous broadening. The steeper slope in the infrared spectra is on the lower frequency side while in the SFG spectra it is on the higher frequency side. This (small) difference indicates a different weighting of intensities in the two spectroscopies. The question of whether the additional broadening is due to vibrational life time or due to dephasing could be addressed only by time-resolved pump-and-probe measurements.

5.3. Conformational changes due to solvents and electrolytes

The absence of CH_2 stretching SFG peaks in electrolyte is probably based on local inversion symmetry in the form of an all-*trans* methylene chain, which suggests a lower defect density than in air. Note that a completely isotropic distribution of CH_2 orientations, which would also result in zero SFG intensity, is unlikely since the molecule is and remains adsorbed. In contrast, SFG spectra for alkanethiolates terminated by CH_3 groups do not change remarkably between environments of air and aqueous solution. SFG could not detect a signal from the CH_2 group for ordered layers, irrespective of whether they were in air or in aqueous electrolytes [5,7,26,27]. The result thus suggests that the effect is most likely due to conformations induced by the presence of the functional groups of AT as is also known for alkoxy-terminated SAMs [9].

We suggest the following scenario: AT layers should be less dense than alkanethiolate layers due to the large functional group (alternatively they could show an extreme tilt and nicely ordered methylene chains, but this would be incompatible with the gauche defects discussed in Section 5.1). Comparable disordered SAM systems are ω-SO_3H– [34] and ω-COOH– [35] alkanethiolates. Thus the solvent may penetrate the layer and the chain extends into the aqueous solution although the backbone is hydrophobic. While the amide should remain unprotonated in the pH range investigated here, the role of the NH_2 group—partially protonated due to the low pH of the HCl solution—is crucial: its position at the tail of the molecule may allow complete solvation by water. The water thus dominates all interchain interactions; multiple hydrogen bonds between the amine and water determine the molecular structure; even ion pairs of the protonated amine with anions are possible. The protonation at low pH should be nearly complete and cause some intermolecular repulsion. We propose to investigate this effect further by applying an electrochemical potential (see also the case of alkanethiolate on platinum [7]). In contrast, alkoxy-terminated SAMs lose their order upon contact with water [9].

When the layer is dried, the molecules can no longer stand up in a low-density phase (or in a tilted and ordered phase), and the chain deforms strongly during the removal of the solvent as the functional group becomes exposed to air. We note that such deformations in one chain should entrain deformations also in neighboring chains, hence operating in a collective way. ν_s and ν_{as} modes of C–H stretching vibrations in the alkyl chain appear in the SFG spectrum. In addition the 'defect peak' appears. The difference from ν_s and ν_{as} is that it is not observed after contact with ethanol. Hence, this peak may point towards some remaining chain disorder after incomplete drying, when the electrolyte or water layer thickness is in the nanometer range (note that this situation corresponds to a macroscopically dry surface). We term this the 'solvent memory effect'. In contrast to ethanol, strongly adsorbed water molecules (or water and ions) may remain on the sample after drying, but such ultrathin layers do not behave in the same way as bulk water, especially concerning solvation of the functional group.

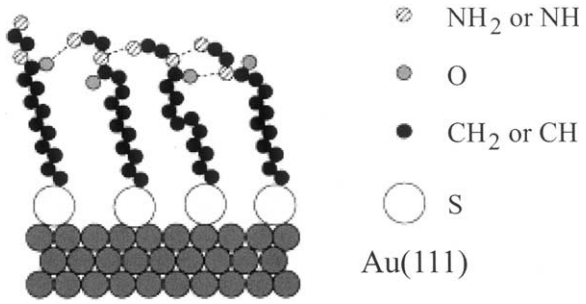

Fig. 6. Model for the dry AT monolayer. Multiple intermolecular hydrogen bonds lead to the deformation of the alkyl backbone.

[1] In some cases, adsorbed ω-mercaptoalkanesulfonic acids show an additional infrared peak at approximately 2960 cm^{-1} (Mandler, personal communication).

Now, in the absence of electrolyte, inter- and maybe intra-molecular hydrogen bonds can form. This is again opposite to the behavior of alkoxy-terminated SAMs [9]. Especially the C=O···H–N bond is strong (usually > 20 kJ mol^{-1}, thus at least four times larger than a methylene–methylene van-der-Waals bond [36]). A single hydrogen bond can thus outweigh the formation energy even for a *cis* conformation, approximately 20 kJ mol^{-1} [36]. We present an illustration for this situation in Fig. 6. A similar effect operates in biomolecules such as peptides, protein and DNA; it ensures the well-known typical 3D structures of biomolecules. We can compare the AT layer with a protein or peptide, where the interaction of amino acid side chain groups with electrolytes (solvation) or with other molecules can lead to preferred backbone conformations, especially β-sheets and α-helices.

However, we do not observe the huge blue shift typical for *cis* conformations, so their concentration must be small. Since our calculations and literature data (see Section 4) show that gauche defects do not result in large spectral changes in the $\nu(CH_2)$ region, the situation is close to that in cyclohexane, i.e. a chain contains multiple gauche defects. In this scenario only a few CH_2 groups would have to be in a position which generates a strong SFG signal. Thus our estimate of one SFG-producing group per molecule fits very well.

The 'solvent memory effect' points towards different molecular geometries, depending on the solvation. It is surprising that the absence or presence of Pd^{2+}, which is known to attach to this molecular layer as a complex [10], does not influence the spectra. When we consider arguments from the typical Pd(II) chemistry [10], especially the facile formation of $PdCl_2(amine)_2$ complexes from $PdCl_4^{2-}$ and amines, we can postulate a clear difference from free ligands in solution: the most likely configuration is not an intra-, but an *inter*-molecular chelate of two AT molecules and a Pd(II) center which does not produce *cis* conformations. Surprisingly, the electrolyte and not the metal ion determines the SAM structure.

6. Conclusions

We investigated a self-assembled thiolate monolayer with amine and amide groups on Au(111) with SFG and infrared spectroscopy. The combination of both techniques, complemented by calculated infrared spectra of model compounds, allows us to draw the following conclusions from shape, intensities and widths of the methylene stretching vibrations.

(1) In situ SFG shows a disappearance of the signals in aqueous electrolytes. We propose that the hydration of the (partially protonated) amine group breaks intermolecular hydrogen bonds and allows the molecule to move towards an all-*trans* conformation. Hence, in solution, the ordering of the layer is very high while the removal of the electrolyte results in a complete and sudden modification of the interface. This principle should operate for a large number of organic adlayer systems that contain hydrogen bonds.

(2) We observed a 'solvent memory effect', i.e. the molecular layers—after having been in contact with a solvent and dried—show bands with a typical fingerprint. Again the different possibilities to form hydrogen bonds and their breakup should cause this phenomenon. Clearly, the SAM is rather flexible, in contrast to simple alkanethiolate SAMs of comparable chain length.

(3) The bonding of Pd(II) ions does not change the conformation, which leads us to postulate an intermolecular chelate, in contrast to the typical intramolecular chelate of bifunctional ligands.

(4) The broadening of the antisymmetric CH_2 stretch in SFG and infrared spectra is extremely large and thus not comparable to that observed in ordered or even disordered alkanethiolate SAMs. It is—differently from that of the symmetric mode—probably due to dephasing. The small blue shift of the bands is compatible with multiple gauche defects like in cyclohexane. Calculations show that the stretching modes in cyclo- and *n*-alkanes are geometrically closely related, and that the defects cause the blue shift.

Acknowledgements

AMB would like to thank the Alexander von Humboldt Foundation for a Feodor Lynen Research Fellowship.

References

[1] F. Schreiber, Prog. Surf. Sci. 65 (2000) 151.
[2] M.J. Giz, B. Duong, N.J. Tao, J. Electroanal. Chem. 465 (1999) 72.
[3] O. Cavalleri, A.M. Bittner, H. Kind, K. Kern, T. Greber, Z. Phys. Chem. 208 (1999) 107.
[4] H. Hagenström, M.A. Schneeweis, D.M. Kolb, Langmuir 15 (1999) 7802.
[5] M. Epple, A.M. Bittner, K. Kuhnke, K. Kern, W.-Q. Zheng, A. Tadjeddine, Langmuir 18 (2002) 773.
[6] A.S. Viana, A.H. Jones, L.M. Abrantes, M. Kalaji, J. Electroanal. Chem. 500 (2001) 290.
[7] M.A. Hines, J.A. Todd, P. Guyot-Sionnest, Langmuir 11 (1995) 493.
[8] M.R. Anderson, M.N. Evaniak, M. Zhang, Langmuir 12 (1996) 2327.
[9] M. Zolk, F. Eisert, J. Pipper, S. Herrwerth, W. Eck, M. Buck, M. Grunze, Langmuir 16 (2000) 5849.
[10] H. Kind, A.M. Bittner, O. Cavalleri, T. Greber, K. Kern, J. Phys. Chem. B 102 (1998) 7582.
[11] GAUSSIAN 98, M.J. Frisch et al., Gaussian Inc, Pittsburgh, PA, 2001.

[12] A. Le Rille, A. Tadjeddine, J. Electroanal. Chem. 467 (1999) 238.
[13] D.M.P. Hoffmann, K. Kuhnke, A.M. Bittner, K. Kern, unpublished.
[14] R.H. Terrill, T.A. Tanzer, P.W. Bohn, Langmuir 14 (1998) 845.
[15] F. Bensebaa, T.H. Ellis, A. Badia, R.B. Lennox, Langmuir 14 (1998) 2361.
[16] P. Harder, M. Grunze, R. Dahint, G.M. Whitesides, P.E. Laibinis, J. Phys. Chem. 102 (1998) 426.
[17] S.E. Creager, C.M. Steiger, Langmuir 11 (1995) 1852.
[18] F.J. Touwslager, A.H.M. Sondag, Langmuir 10 (1994) 1028.
[19] M.A. Bryant, J.E. Pemberton, J. Am. Chem. Soc. 113 (1993) 3629.
[20] M.A. Bryant, J.E. Pemberton, J. Am. Chem. Soc. 113 (1993) 8284.
[21] R.G. Snyder, S.L. Hsu, S. Krimm, Spectrochim. Acta 34A (1978) 395.
[22] J.P. Rabe, J.D. Swalen, J.F. Rabolt, J. Chem. Phys. 83 (1987) 1601.
[23] P.T.T. Wong, T.E. Chagwedera, H.H. Mantsch, J. Chem. Phys. 87 (1987) 4487.
[24] M. Osawa, K. Ataka, K. Yoshii, Y. Nishikawa, Appl. Spectr. 47 (1993) 1497.
[25] R.N. Ward, D.C. Duffy, P.B. Davies, C.D. Bain, J. Phys. Chem. 98 (1994) 8536.
[26] M. Himmelhaus, F. Eisert, M. Buck, M. Grunze, J. Phys. Chem. B 104 (2000) 576.
[27] N. Akamatsu, K. Domen, C. Hirose, J. Phys. Chem. 97 (1993) 10070.
[28] B. Schrader, Raman/Infrared Atlas of Organic Compounds, Verlag Chemie, Weinheim, 1989.
[29] R.W. Berg, K. Rasmussen, Spectrochim. Acta 29A (1973) 319.
[30] R.W. Berg, K. Rasmussen, Spectrochim. Acta 28A (1972) 2319.
[31] J.J. Kharitonov, H. Bissinger, E. Ambach, W. Beck, Z. Naturforsch. 73b (1982) 1034.
[32] S. Pan, A.M. Belu, B.D. Ratner, Mater. Sci. Eng. C7 (1999) 51.
[33] R.G. Snyder, M. Maroncelli, H.L. Strauss, V.M. Hallmark, J. Phys. Chem. 90 (1986) 5623.
[34] I. Turyan, D. Mandler, Israel J. Chem. 37 (1997) 225.
[35] O. Dannenberger, K. Weiss, H.-J. Himmel, B. Jäger, M. Buck, Ch. Wöll, Thin Solid Films 307 (1997) 183.
[36] A. Streitwieser, C.H. Heathcock, Organische Chemie, Verlag Chemie, Weinheim, 1986.
[37] D. Lin-Vien, N.B. Colthup, W.G. Fateley, J.G. Grasselli, Infrared and Raman Frequencies of Organic Molecules, Academic Press, San Diego, 1991.